ELSEVIER

Splitting Tension Tests to Determine Concrete Fracture Parameters by Peak-Load Method

Sungchul Yang,* Tianxi Tang,† Dan G. Zollinger,* and Ashok Gurjar*
*Texas A & M University, College Station; and †Texas Transportation Institute, College Station, Texas

An experimental program confirms that the peak-load method can be successfully applied to splitting tension tests to determine fracture parameters K_{Ic}^S *and* $CTOD_c$ *of the two-parameter fracture model from the measured peak loads. The peak-load method requires distinct specimens. It is found that a hole drilled at the axis of splitting tension cylinder can largely expand the specimen distinction. Combination of tests on splitting tension cylinders with and without a hole raises the reliability of the* K_{Ic}^S *and* $CTOD_c$ *values determined by the peak-load method.* © 1997 Elsevier Science Ltd. ADVANCED CEMENT BASED MATERIALS 1997, 5, 18–28

KEY WORDS: Beam bending, Concrete, Eccentric compression, Fracture mechanics, Peak load, Splitting tension, Statistics, Strength, Test method, Two-parameter fracture model

According to the two-parameter fracture model (TPFM) [1], a concrete structure fails when the stress intensity factor K_I and the crack tip opening displacement ($CTOD$) reach their critical values, K_{Ic}^S and $CTOD_c$, simultaneously. Since both K_I and $CTOD$ can be calculated with linear elastic fracture mechanics (LEFM), this fracture model can be easily applied to structural analysis and design. Therefore, experimental determination of K_{Ic}^S and $CTOD_c$ is a key issue. RILEM [2] has recommended a test method for determining these parameters. The recommended test requires a closed-loop testing system to measure the initial compliance and the compliance at the peak load. This testing facility requirement has restricted the use of the two-parameter fracture model, because a closed-loop testing system is not available in many laboratories and work sites. To overcome the restriction, Tang et al. [3] proposed a simple method, named the peak-load method, for determining K_{Ic}^S and $CTOD_c$. With this new method, only peak loads of several distinct specimens need to be measured. Then Tang et al. [4] introduced two quantities to evaluate the statistics involved in the peak-load method so that specimens can be designed to be considerably distinct for reliable results.

Three-point bend beams have been widely used to measure fracture properties of concrete. The test procedure that RILEM recommended also proposes using this type of specimen. It has been found that both the beam size and notch length can enlarge the distinction between specimens in the peak-load method. Besides, different load conditions can also provide considerable distinction between specimens.

The cylindrical specimen is another type of specimen that can be easily molded (ASTM C31 and C192). It can also be taken from existing structures by core drilling (ASTM C42). Splitting tension of the cylindrical specimen is a common test for evaluating indirect tensile strength (ASTM C496). By making a notch along a diameter of the cylinder, researchers have used the splitting tension test to study fracture behavior of concrete. This paper reports an investigation on the use of splitting tension fracture tests by the peak-load method. It is shown by finite element analysis that a hole drilled at the axis of the notched splitting tension cylinder significantly changes the fracture intensity factor K_I and crack opening displacement (COD). As a result, splitting tension cylinders with holes are appreciably distinct from those cylinders without holes in the sense of the peak-load method. A series of tests conducted in the study show that combination of tests on splitting tension cylinders with and without holes increases the reliability of K_{Ic}^S and $CTOD_c$ values determined by the method.

Review of Peak-Load Method for Two-Parameter Fracture Model

The critical stress intensity factor K_{Ic}^S and the critical crack tip opening displacement $CTOD_c$ uniquely deter-

Address correspondence to: Tianxi Tang, Texas Transportation Institute, TTI/CE Building, Suite 508, College Station, Texas 77843.
Received September 29, 1995; Accepted July 23, 1996

ISSN 1065-7355/97/$17.00
PII S1065-7355(96)00074-0

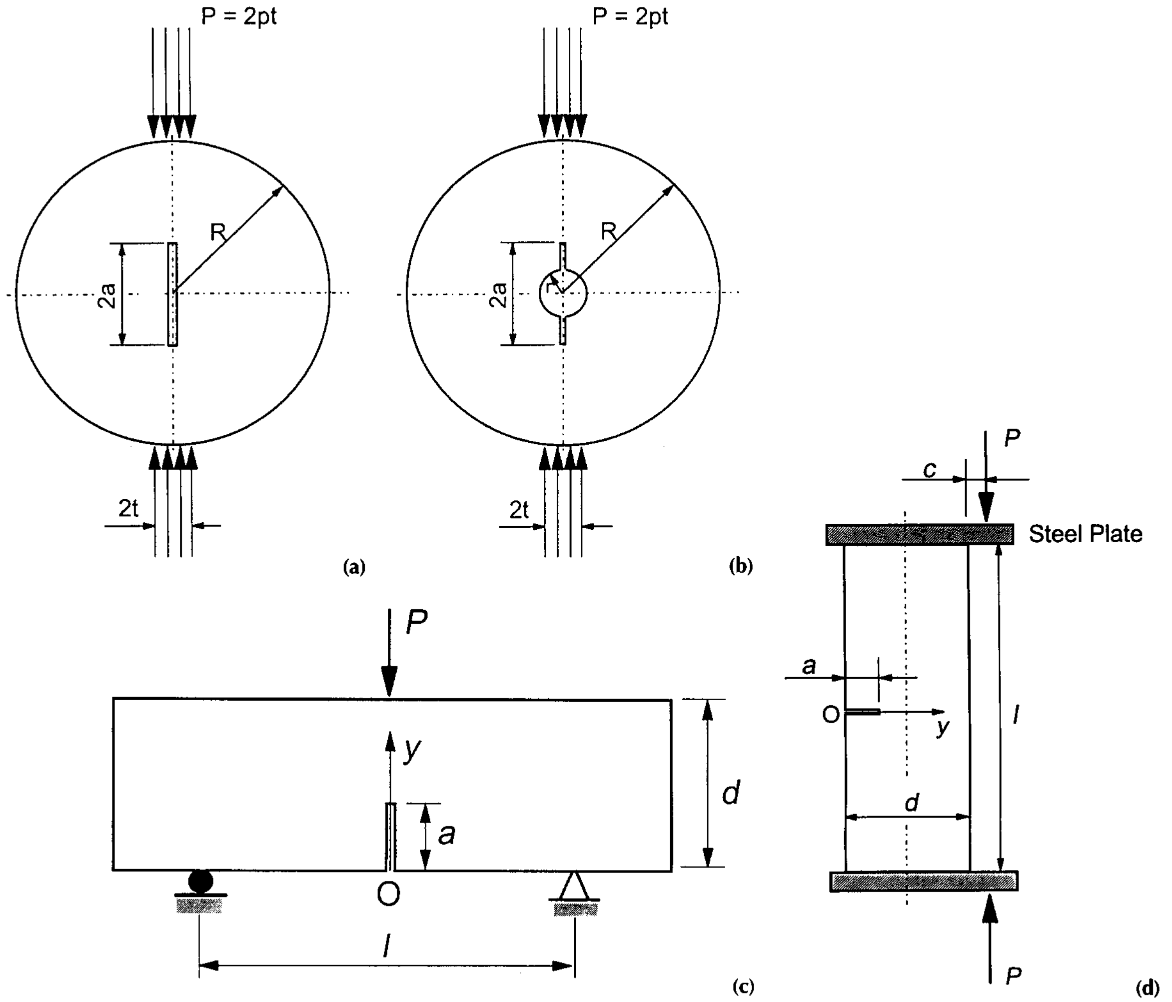

FIGURE 1. Fracture test specimens. (a) Regular splitting tension cylinder; (b)holed splitting tension cylinder; (c) three-point bend beam; (d) eccentric compression prism.

mine the critical nominal stress σ_{Nc} and the critical effective crack length a_c [1]. The failure criterion of a concrete structure is then simultaneous satisfaction of the following two equations:

$$K_I(\sigma_{Nc}, a_c) = K_{Ic}^S \tag{1}$$

$$CTOD(\sigma_{Nc}, a_c) = CTOD_c \tag{2}$$

where the quantities on the left sides of eqs 1 and 2 can be expressed through an analytical or numerical solution based on LEFM. Solutions of K_{Ic}^S and $CTOD_c$ from measured σ_{Nc} values through eqs 1 and 2 are the basis of peak-load method. A review of this method [3,4] is give as follows.

When eqs 1 and 2 are applied to two distinct specimens, four equations are obtained. If critical nominal stresses for the two specimens are measured, four unknowns, K_{Ic}^S, $CTOD_c$, and the critical effective crack lengths (a_c^1 for specimen 1 and a_c^2 for specimen 2), can be

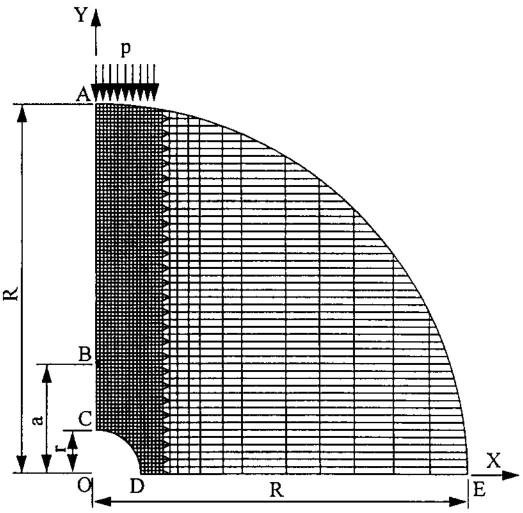

FIGURE 2. Finite element mesh for holed splitting tension cylinder.

Advn Cem Bas Mat
1997;5:18–28

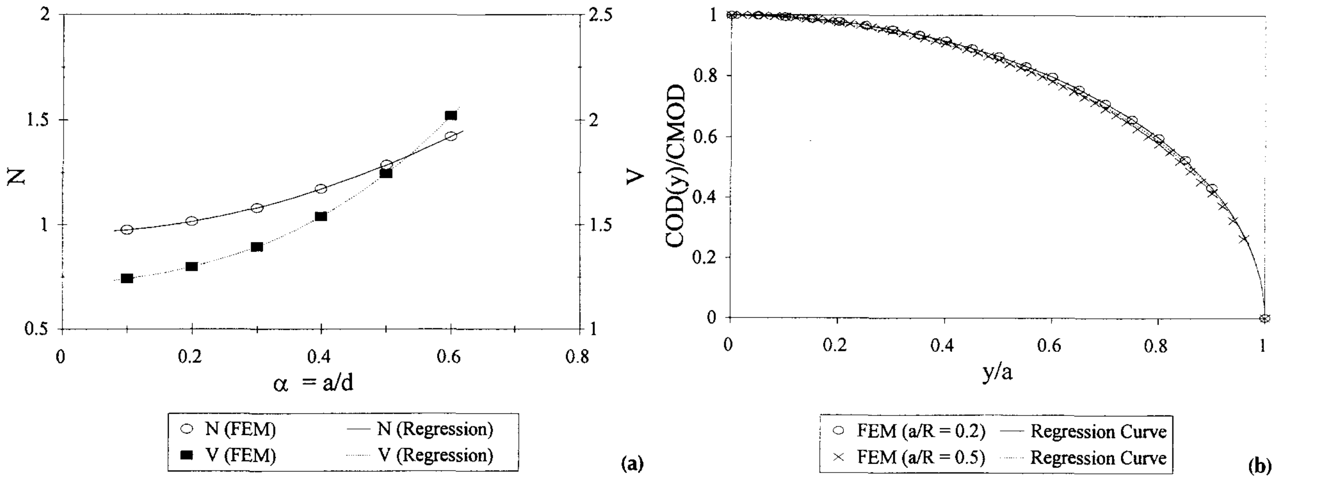

FIGURE 3. (a) $N(\alpha)$ and $V(\alpha)$ for regular splitting tension cylinder. (b) Crack profiles for regular splitting tension cylinder. COD = crack opening displacement; CMOD = crack mouth opening displacement.

solved through the four equations. Although the solution of K^S_{Ic} and $CTOD_c$ may be mathematically possible from the peak loads of two distinct specimens, three or more specimens must be tested to reduce random errors.

For each of the specimens tested, TPFM gives that

$$K_I(\sigma^i_{Nc}, a^i_c) = K^S_{Ic} \quad (3)$$

$$CTOD(\sigma^i_{Nc}, a^i_c) = CTOD_c \quad (4)$$

when the specimen fails. Superscript i denotes the ith specimen. Combinations of eqs 3 and 4 with a^i_c as the parameter can be considered the parametric form of a function for $CTOD_c$ in terms of K^S_{Ic}. The Cartesian form of the function is

$$CTOD_c = CTOD^i(K^S_{Ic}). \quad (5)$$

If there were no random errors, all the $CTOD_c$ – K^S_{Ic} curves would meet at the same point to give the "exact" solution K^S_{Ic} and $CTOD_c$. Because randomness of concrete properties and errors of measurement always exists, three or more distinct specimens need to be tested for statistically valid results. From TPFM (eqs 1 and 2), the critical nominal stress is determined by K^S_{Ic} and $CTOD_c$:

$$\sigma^i_{Nc} = \phi^i(K^S_{Ic}, CTOD_c). \quad (6)$$

Independent of each other, K^S_{Ic} and $CTOD_c$ can be determined by minimization of

$$\Phi(CTOD_c, K^S_{Ic}) = \sum_{i=0}^{n} w_i[(\sigma_{Nc})^i - \phi^i(K^S_{Ic}, CTOD_c)]^2 \quad (7)$$

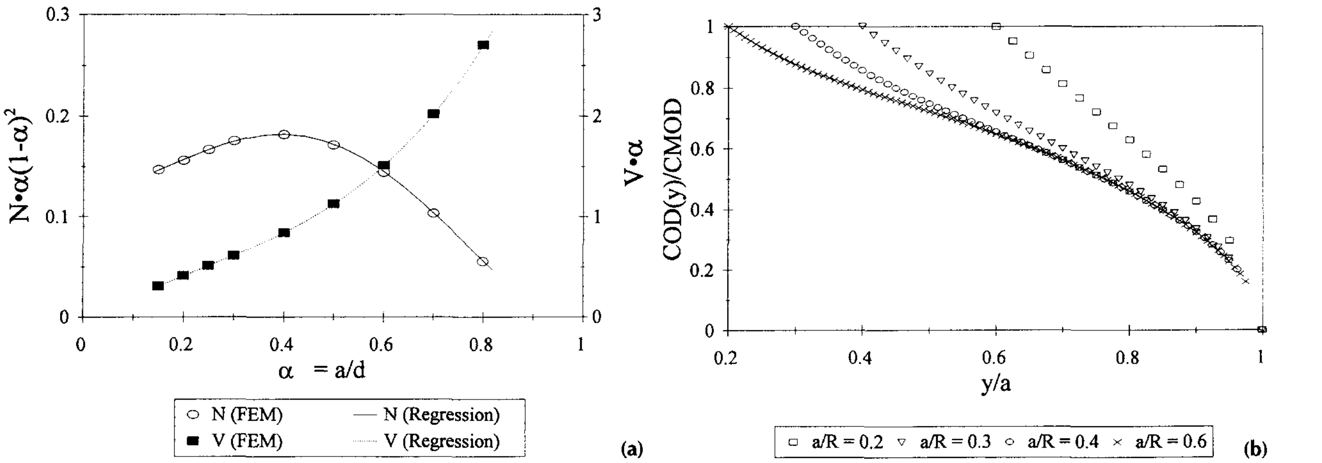

FIGURE 4. (a) $N(\alpha)$ and $V(\alpha)$ for holed splitting tension cylinder ($r/R = 0.08$). (b) Crack profiles for holed splitting tension cylinder ($r/R = 0.08$). COD = crack opening displacement; CMOD = crack mouth opening displacement.

TABLE 1. Regression coefficients L_0, L_1, L_2, and L_3 for eq 23

		$\alpha = a/R$						
r/R	**Coefficient**	**0.2**	**0.3**	**0.4**	**0.5**	**0.6**	**0.7**	**0.8**
0.08	L_0	2.3595	1.7016	1.4054	1.2533	1.1647	1.1076	1.0724
	L_1	−5.4530	−3.7623	−2.7499	−2.0855	−1.6124	−1.2499	−0.9825
	L_2	6.4461	5.0238	3.9642	3.1257	2.4360	1.8553	1.4143
	L_3	−3.2118	−2.8291	−2.4859	−2.1596	−1.8573	−1.5905	−1.3982
0.12	L_0	4.2222	2.4074	1.8462	1.5478	1.3683	1.2664	1.1836
	L_1	−10.7400	−5.7126	−4.1700	−3.1765	−2.4591	−2.0179	−1.5656
	L_2	12.3770	6.9096	5.4374	4.397	3.4445	2.8996	2.2137
	L_3	−5.7009	−3.4722	−2.9870	−2.5973	−2.2344	−2.0466	−1.7436

as a two-variable optimization, where n is the total number of specimens and w_i are weights. The peak-load method simplifies the problem to a one-variable optimization problem taking K_{Ic}^S as the single variable but $CTOD_c$ determined by K_{Ic}^S with the measured σ_{Nc} (eq 5). It solves K_{Ic}^S by minimizing the following function:

$$f(K_{Ic}^S) = \sum_{i=1}^{n} (CTOD_c^{avg} - CTOD_c^i)^2 \tag{8}$$

where $CTOD_c^i$ are functions of K_{Ic}^S (eq 5) and $CTOD_c^{avg}$ is the average of $CTOD_c^i$ of all n specimens for the same K_{Ic}^S value. The value of K_{Ic}^S at which the minimum of f occurs is the solution of material parameter K_{Ic}^S, designated by K_{Ic}^S*. By substituting K_{Ic}^S* into the $CTOD_c^{avg} - K_{Ic}^S$ curve, the solution of $CTOD_c$, designated by $CTOD_c*$ is obtained. The asterisk indicates the values determined by the peak-load method. The simplification is based on various experimental results, which have shown that values of K_{Ic}^S for a given concrete obtained from different specimens with the compliance method are much closer to one another than those of $CTOD_c$ [5]. Although the two-variable optimization (eq 7) is more strict than the one-variable optimization (eq 8) from a statistical point of view, the latter provides a very simple search procedure. Tests have shown [3] that the K_{Ic}^S and $CTOD_c$ values determined by the peak-load method are very close to those measured by the compliance method, the test method recommended by RILEM [2].

It is important to point out that the statistics involved in the peak-load method is not only to average the data scatter due to randomness of material properties and errors in measurement but to select an average value of $CTOD_c$ whose variance is the least among all the possible values of $CTOD_c$ for different specimens. When all the specimens are identical in geometry and size, the differences between the $CTOD_c - K_{Ic}^S$ curves of these specimens are caused by randomness only, and therefore K_{Ic}^S and $CTOD_c$ cannot be determined by a statistics procedure. To use the peak-load method, one should ensure that the test specimens are so distinct that the differences between the curves are not significantly influenced by the random errors. In minimizing f to obtain K_{Ic}^S* and $CTOD_c*$, the values so determined are of high reliability when the increment of f from the minimum f, Δf, is high for a given small ΔK_{Ic}^S. The second-order approximation of Δf can be expressed in the form of

$$\Delta f = \frac{1}{2}\frac{d^2 f}{(dK_{Ic}^S)^2}(\Delta K_{Ic}^S)^2 \tag{9}$$

since $df/dK_{Ic}^S = 0$ at the minimum f. Another approach of the second-order approximation of Δf can be obtained by substituting the first-order approximation of $\Delta CTOD_c^i$ in terms of ΔK_I^S into eq 8, that is,

$$\Delta f = \beta(\Delta K_{Ic}^S)^2 \ or \ \beta = \frac{\Delta f}{(\Delta K_{Ic}^S)^2} \tag{10}$$

where

$$\beta = \sum_{i=1}^{n} (k^{avg} - k^i)^2, \tag{11}$$

$$k = \left[\frac{dCTOD_c}{dK_{Ic}^S}\right]_{K_{Ic}^{S*}} \tag{12}$$

TABLE 2. Mix designs of concrete (for 1-m^3 of concrete)

Content	Mix *B* (kg)	Mix *D* (kg)
Cement (type I)	391	251
Fly ash (type C)	—	68
Coarse aggregate (crushed limestone)	1055	684
Intermediate aggregate (siliceous sand)	—	399
Fine aggregate (siliceous sand)	721	765
Water	204	134

Note: The maximum size of the coarse aggregate is 9.5 mm for mix *B* and 25.4 mm for mix *D*.

TABLE 3. Test data of split tension cylinders of concrete batch B

Specimen Group No.	Test No.	Dimensions (mm)		a_0 (mm)	r/R	P_{max} (N)	Average P_{max} (N)	k (10^{-4} $m^{1/2}$/MPa)
		b	R					
Group 1	B-ST1	63.0	76.2	9.0	0	47860	49370	0.237
	B-ST2	63.0	76.2	10.0	0	46750		
	B-ST3	60.0	76.2	9.0	0	53510		
Group 2	B-ST4	74.0	76.2	19.8	0.12	42930	40300	0.284
	B-ST5	77.0	76.2	18.8	0.12	37320		
	B-ST6	78.0	76.2	19.0	0.12	40660		
Group 3	B-ST7	77.0	76.2	34.5	0.12	27890	25040	0.692
	B-ST8	76.0	76.2	34.3	0.12	22600		
	B-ST9	75.0	76.2	34.3	0.12	24640		

Note: The k value is calculated at K_{Ic}^{S*} = 1.043 MPA · $m^{1/2}$.

subscript K_{Ic}^{S*} indicates that k is calculated at K_{Ic}^{S*}, and k^{avg} is the average of the k^i values of all the specimens. For any given ΔK_{Ic}^S, β is proportional to Δf. Therefore, β is a measure for distinction of all the specimens in the sense of peak-load method. It was referred to as the confidence level of K_{Ic}^S and $CTOD_c$ determined by the peak-load method in the previous work [4]. Comparison of eqs 9 and 10 indicates that the quantity β is equal to half the curvature of the $f - K_{Ic}^S$ curve at the minimum f. To avoid confusion with the term "confidence level" traditionally used for a different quantity in statistics, we can just define β as half the curvature of the $f - K_{Ic}^S$ curve at the minimum f or K_{Ic}^{S*}. Since β can be calculated from the slope of the $CTOD_c - K_{Ic}^S$ curve at K_{Ic}^{S*}, designated as k (eq 11), specimens can be approximately distinguished by the value of k in the sense of the peak-load method. By observing LEFM formulas for K_I and $CTOD$, one can find how k depends on specimen geometry, specimen size, and notch length. With β and k, specimens can be designed to be largely distinct so as to achieve reliable results for K_{Ic}^S and $CTOD_c$.

Analyses of Different Specimen Geometries

Finite element analysis (FEA) on the regular split tension cylinder (Figure 1a) and the holed split tension cylinder with an initial notch (Figure 1b) was performed by using the program package ABAQUS. Here the word "regular" refers to the splitting tension cylinder with no hole drilled in it, whereas "holed" refers to that cylinder with a drilled hole. Specimen geometries are carefully meshed. Figure 2 shows the mesh for the holed specimen where the ratio of the hole radius to the specimen radius is r/R = 0.12. By considering the effect of the load-bearing width [6], one assumes the load is distributed over t/R = 0.16. Based on the data output from FEA, LEFM formulas for K_I, crack mouth opening displacement $CMOD$, and COD profiles are developed by the least squares method.

Regular Splitting Tension Cylinder

Based on the FEA results, the stress intensity factor K_I can be expressed as follows:

$$K_I = \sigma_N \sqrt{\pi a} N(\alpha) \tag{13}$$

where σ_N is the nominal stress:

$$\sigma_N = \frac{P}{\pi b R} \tag{14}$$

TABLE 4. Test data of three-point beam of concrete batch B

Specimen Group No.	Test No.	Dimensions (mm)		a_0 (mm)	l/d	P_{max} (N)	Average P_{max} (N)	k (10^{-4} $m^{1/2}$/MPa)
		d	b					
Group 1	B-BG1	152.4	152.4	12.8	2.5	26420	26375	0.439
	B-BG2	152.4	152.4	14.3	2.5	26330		
Group 2	B-BG3	152.4	152.4	26.3	2.5	20190	20725	0.556
	B-BG4	152.4	152.4	25.8	2.5	21260		
Group 3	B-BG5	152.4	152.4	37.7	2.5	17880	17280	0.606
	B-BG6	152.4	152.4	37.5	2.5	16680		

Note: The k value is calculated at K_{Ic}^{S*} = 1.043 MPa · $m^{1/2}$.

TABLE 5. Test data of eccentric compression prisms of concrete batch B

Test No.	Dimensions (mm)		a_0 (mm)	c/d	l/d	P_{max} (N)	k (10^{-4} $m^{1/2}$/MPa)
	d	b					
B-EC1	157	151	16.5	1/24	2	37280	0.660
B-EC2	156	152	41.7	1/24	2	29450	0.998
B-EC3	150	150	56.0	1/24	2	27130	1.280

Note: The k value is calculated at K_{Ic}^{S*} = 1.043 MPa · $m^{1/2}$.

$N(\alpha)$ is the geometry factor:

$$N(\alpha) = 0.964 - 0.026\alpha + 1.472\alpha^2 - 0.256\alpha^3 \quad (15)$$

a is the crack length, α is a/R, R is the radius of the cylinder specimen, P is the total compressive load, and b is the length of the cylinder. Values of the stress intensity factor K_I for α from 0.1 to 0.6 are obtained through the J integral, from which eq 15 is obtained by regression. $N(\alpha)$ values determined from the FEA do not deviate from eq 15 by more than 0.5% (Figure 3a).

Another geometry function $V(\alpha)$ for the regular splitting tension cylinder is obtained for the $CMOD$ (Figure 3a):

$$CMOD = \frac{\pi a \sigma_N}{E'} V(\alpha) \quad (16)$$

$$V(\alpha) = 1.215 + 0.171\alpha + 0.906\alpha^2 + 1.745\alpha^3 \quad (17)$$

where $E' = E/(1 - \nu^2)$ for plane strain and $E' = E$ for plane stress, E is the elastic modulus, and ν is Poisson's ratio. Equation 17 fits all the data points from the finite element analysis data very well with the square of the sample correlation coefficient R^2 larger than 0.99999.

The COD profile (Figure 3b) is given in a form similar to that for a bend beam provided by Jenq and Shah [1]:

$$\frac{COD(y)}{CMOD} = \sqrt{\left(1 - \frac{y}{a}\right)^2 + [2.048 - 0.27\alpha]\left[\frac{y}{a} - \left(\frac{y}{a}\right)^2\right]}. \quad (18)$$

Equation 18 is derived for the range of α from 0.1 to 0.5. The largest deviation of the values given by eq 18 from the FEA results appears in the case of $\alpha = 0.5$ and $y/a > 0.84$. The deviation is less than 2%.

Holed Splitting Tension Cylinder

The FEA results show that a hole drilled at the specimen center changes the stress distribution in the split tension cylinder dramatically. Holes of two different sizes are investigated: $r/R = 0.08$ and $r/R = 0.12$. Figure 2 shows the FEA mesh for the specimen with $r/R = 0.12$. Functions of $N(\alpha)$ and $V(\alpha)$ for the holed splitting tension cylinder with $r/R = 0.08$ obtained based on the FEA computation (Figure 4a) are

$$N(\alpha) = \frac{0.129 - 0.039\alpha + 1.496\alpha^2 - 3.394\alpha^3 + 1.802\alpha^4}{(1 - \alpha)^2 \alpha} \quad (19)$$

$$V(\alpha) = \frac{-0.046 + 2.75\alpha - 3.28\alpha^2 + 4.6\alpha^3 + 0.7\alpha^4}{\alpha}. \quad (20)$$

It should be noted that these regression functions $N(\alpha)$ and $V(\alpha)$ are based on their values at α = 0.15, 0.2, 0.25, 0.3, 0.4, 0.5, 0.6, 0.7, and 0.8. None of the $N(\alpha)$ values deviate from eq 19 by more than 0.5% and none of the $V(\alpha)$ values deviate from eq 20 by more than 1%.

Functions of $N(\alpha)$ and $V(\alpha)$ for the holed split tension cylinder with $r/R = 0.12$ are

TABLE 6. Test data of split tension cylinders of concrete batch D

Specimen Group No.	Test No.	Dimensions (mm)		a_0 (mm)	r/R	P_{max} (N)	k (10^{-4} $m^{1/2}$/MPa)
		b	R				
Group 1	D-ST1	74.0	76.2	10.5	0	43190	0.348
	D-ST2	74.5	76.2	10.0	0	36920	0.384
Group 2	D-ST3	73.8	76.2	20.9	0.08	31320	0.422
	D-ST4	76.3	76.2	21.0	0.08	33010	0.418
Group 3	D-ST5	76.3	76.2	30.5	0.08	23890	0.636
	D-ST6	73.3	76.2	30.5	0.08	30600	0.537

Note: The k value is calculated at K_{Ic}^{S*} = 0.847 MPA · $m^{1/2}$.

TABLE 7. Test data of three-point beam of concrete batch D

Specimen Group No.	Test No.	Dimensions (mm)		a_0 (mm)	l/d	P_{max} (N)	k (10^{-4} $m^{1/2}$/MPa)
		d	b				
Group 1	D-BG1	101.6	76.2	12.0	2.5	6270	0.586
	D-BG2	101.6	76.2	12.0	2.5	6630	0.575
Group 2	D-BG3	101.6	76.2	27.5	2.5	4630	0.606
	D-BG4	101.6	76.2	28.5	2.5	4580	0.607
Group 3	D-BG5	101.6	76.2	39.5	2.5	3560	0.585
	D-BG6	101.6	76.2	39.5	2.5	3600	0.587

Note: The k value is calculated at K_{Ic}^{S*} = 0.847 MPa · $m^{1/2}$.

$$N(\alpha) = \frac{0.255 - 0.713\alpha + 3.1\alpha^2 - 5.16\alpha^3 + 2.52\alpha^4}{(1-\alpha)^2\alpha} \quad (21)$$

$$V(\alpha) = \frac{-0.472 + 6.2\alpha - 8.82\alpha^2 + 10.86\alpha^3 + 2.52\alpha^4}{(1+\alpha)\alpha}. \quad (22)$$

The regression functions $N(\alpha)$ and $V(\alpha)$ are based on their values at α = 0.17, 0.2, 0.25, 0.3, 0.4, 0.5, 0.6, 0.7, and 0.8. $N(\alpha)$ values do not deviate from eq 21 by more than 0.4% except that the error is 0.8% at α = 0.8. $V(\alpha)$ values do not deviate from eq 22 by more than 1.5%.

The *COD* profile in the presence of hole is far different from that for the regular splitting tension specimen. A third-degree polynomial in y/a is fitted to $COD(y)/CMOD$ data by using the least squares method (Figure 4b). The general form of the equation is

$$\frac{COD(y)}{CMOD} = L_0(\alpha) + L_1(\alpha)\frac{y}{a} + L_2(\alpha)\left(\frac{y}{a}\right)^2 + L_3(\alpha)\left(\frac{y}{a}\right)^3 \quad (23)$$

where regression coefficients $L_0(\alpha)$, L_1 (α), $L2$ (α), and L_3 (α) are functions of α, and their values for several α are listed in Table 1. The square of the sample correlation coefficient R^2 is between 0.9989 and 0.9999 for all the curve fitting.

Experimental Program

An experimental program was conducted to determine K_{Ic}^S and $CTOD_c$ with splitting tension cylinders of the geometries that are analyzed in the previous discussion. Two batches of concrete cylinders were prepared. Specimens of mix B were made in the laboratory. This mix contained seven sacks (294 kg) of cement per cubic yard (0.765 m^3) of concrete. Mix D concrete specimens used 5.7 sacks (239 kg) of cementitious materials (type I cement plus type C fly ash) per cubic yard of concrete. Specimens of mix D were cast at a construction site located at Hempstead, Texas. Mix proportions for both mix designs are shown in Table 2. The maximum size of

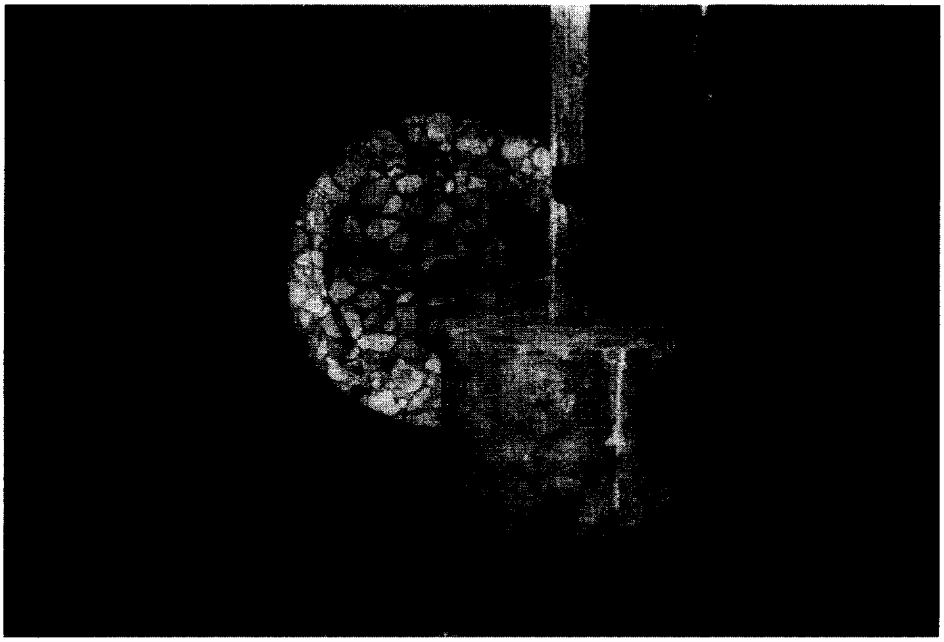

FIGURE 5. Sawing a notch on a splitting tension cylinder by a reciprocal saw machine.

TABLE 8. K^S_{Ic} and $CTOD_c$ values determined from different specimens of batch B

Specimens	K^S_{Ic} (MPa · √m)	$CTOD_c$ (mm)	β (10^{-4} m/GPa²)	Note
Bending	1.036	0.0115	0.147	Based on average peak loads of three specimen groups
Eccentric compression	1.129	0.0235	1.927	Based on peak loads of three tests
Bending and eccentric compression	1.047	0.0138	5.053	Based on average peak loads of total six specimen groups
Split tension	0.842	0.0091	1.252	Based on average peak loads of three specimen groups
Bending, eccentric compression, and split tension	1.043	0.0145	8.786	Based on average peak loads of total nine specimen groups

Note: All the values of β are calculated at $K_{SIc}{}^* = 1.043$ MPa · $m^{1/2}$.

the coarse aggregate for mix B was 12.7 mm, whereas that for mix D was 25.4 mm.

Prism specimens were also prepared from batch B. These specimens were tested in bending (Figure 1c) and eccentric compression (Figure 1d), so that K^S_{Ic} and $CTOD_c$ obtained from them can be used for comparison with the results from the splitting tension cylinders. The LEFM formulas for bending and eccentric compression of prism specimens are included in the Appendix. All the cylinder and prism specimens were demolded 1 day after casting and then cured in a moisture chamber for 28 days. Prism specimens were also prepared from batch D. These specimens were tested in bending. After curing at the construction site for 3 days, specimens from batch D were delivered to a moisture chamber and were cured for 8 days. Besides the fracture specimens from each concrete mix, one cylindrical specimen was tested for compressive strength, from which the elastic modulus was calculated using the American Concrete Institute formula. It was found that the elastic modulus was 26.5 GPa for batch B and 18.8 GPa for batch D.

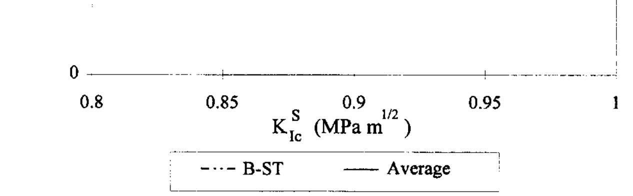

FIGURE 6. $CTOD_c$ – K^S_{Ic} curves for splitting tension cylinders of concrete mix B and their average. CTOD = crack tip opening displacement.

Dimensions of all specimens, along with other test data, are shown in Tables 3 to 7. The specimens were notched just before testing. Beam and eccentric compression specimens were notched by a diamond saw, whereas splitting tension cylinders were notched by a reciprocal saw after a hole was drilled at the specimen center, through which the saw blade was threaded. The blade of the reciprocal saw moved up and down to cut the notch. Figure 5 shows the reciprocal saw in action, along with a holed cylinder with a finished notch. All splitting tension cylinders were 152.4 mm in diameter. For some cylinders, the hole was so fine that it did not have any appreciable influence on the stress distribution around the crack tip. These specimens were treated as regular splitting tension cylinders (Figure 1a). For other splitting tension cylinders (Figure 1b), a hole of 18.3 mm diameter (r/R = 0.12) was drilled for batch B. The hole for the holed specimens from batch D was 12.7 mm in diameter (r/R = 0.08). The width of all the notches was 3 mm. To reduce measurement errors, the length of notch in every specimen was remeasured after the specimen was tested. This was done at three different locations along the specimen thickness, and the average value was taken for data analysis.

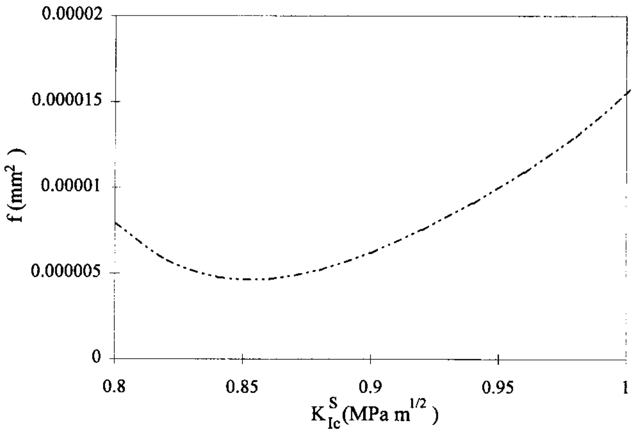

FIGURE 7. f – K^S_{Ic} curve for splitting tension cylinders of mix B.

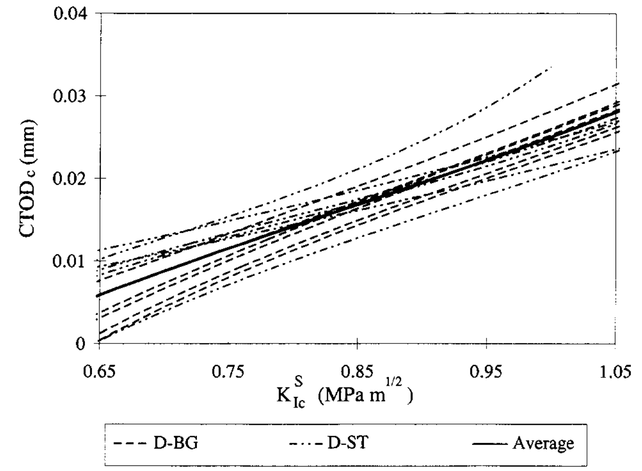

FIGURE 8. $CTOD_c$ - K^S_{Ic} curves of all the specimens of mix D and their average. CTOD = crack tip opening displacement.

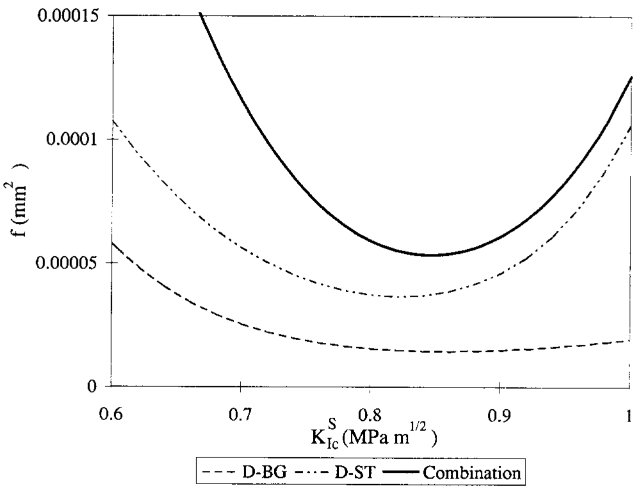

FIGURE 9. f - K^S_{Ic} curves for beams, splitting tension cylinders, and all the specimens of mix D.

Results and Discussion

All fracture tests were conducted with a Tenius-Olsen testing machine. The peak-load method was applied to all the specimens from batch B in groups. All specimens in a group have the similar geometry and same size. The average peak load and dimensions were calculated for each specimen group. The advantage of grouping specimens is a reduction in mathematical manipulations, but either β or k value on the basis of specimen groups is only meaningful for comparison under similar conditions, for example, each group of the same number of specimens. Thus, the $CTOD_c$ − K^S_{Ic} curve is obtained for each of the three groups in each test series.

Table 8 summarizes values of K^S_{Ic} and $CTOD_c$ for batch B obtained by the peak-load method. Specimen groups from either beam bending, eccentric compression, or splitting tension provided close values of K^S_{Ic} and $CTOD_c$. The $CTOD_c$ − K^S_{Ic} curves for all three splitting tension cylinders and their average are shown in Figure 6. The corresponding f − K^S_{Ic} curve is shown in Figure 7. The solutions K^S_{Ic}* and $CTOD_c$* are determined at the minimum f. It is worthwhile to note that when α > 0.8, $K_I(\alpha)$ for the holed cylinder (r/R = 0.08 or 0.12) decreases with increasing α, that is, the specimen geometry is negative. It is suggested that α_0 should not be larger than 0.45 so that the ratio of the critical effective crack length $2\alpha_c$ to the specimen diameter D, $\alpha_c = 2a_c/D = a_c/R$, will not exceed 0.8.

The solutions of K^S_{Ic} and $CTOD_c$ determined from the three different types of specimen are K^S_{Ic} = 1.043 MPa · m$^{1/2}$ and $CTOD_c$ = 0.0145 mm. Based on the solution K^S_{Ic} = 1.043 MPa · m$^{1/2}$, the k value for each specimen is calculated and tabulated in Tables 3 to 5. The values of k for eccentric compression, beam bending, and splitting tension tests are noticeably distinct. Splitting tension provides a higher β value than beam bending (Table 8). The same is true of specimens from mix D. However, a combination of different types of specimens can significantly enhance the β value (Table 8).

The numbers of specimens from batch D are the same for splitting tension and beam bending. The peak-load method was applied to the splitting tension specimens and the beam specimens individually. Figure 8 presents $CTOD_c$ − K^S_{Ic} curves of all the individual specimens and their average. The f − K^S_{Ic} curves shown in Figure 9 are constructed for bend beams, splitting tension cylinders, and a combination of the two. Test data and results are tabulated in Tables 6 and 7. As shown in Table 9, splitting tension provides a higher β value than beam bending. This comparison is more meaningful than that provided by Table 8, because the numbers of beams and cylinders from mix D are equal.

TABLE 9. Values of K^S_{Ic} and $CTOD_c$ determined from different specimens of mix D

Specimens	K^S_{Ic} (MPa · √m)	$CTOD_c$ (mm)	β (10^{-4} m/GPa^2)	Note
Bending	0.857	0.0169	0.008	Based on peak loads of six tests
Split tension	0.823	0.0160	0.584	Based on peak loads of six tests
Bending and split tension	0.847	0.0167	1.127	Based on peak loads of twelve tests

Note: All the values of β are calculated with K^S_{Ic}* = 0.847 MPa · m$^{1/2}$.

TABLE 10. Comparison of k values obtained by different types of specimens

Types of Specimens	Concrete Mix	Minimum k	Maximum k	Max d/Min d	Max α_0/Min α_0	Max k/Min k
Bend beams	B	0.606	0.439	1.0	3.1	1.38
	D	0.607	0.575	1.0	3.3	1.06
Eccentric compression prisms	B	1.280	0.666	1.0	3.4	2.92
Splitting tension cylinders	B	0.692	0.237	1.0	3.5	2.92
	D	0.636	0.348	1.0	2.9	1.83
	Ref [3]	0.230	0.171	1.0	2.5	1.35

Although the k value depends on the specimen size, all the cylinders in this test program had the same size. It is most convenient to prepare cylindrical specimens of the same size in the field. To show how to obtain k values of a large range for specimens of the same size, we summarized some data in Table 10. The ratio of the maximum k value to the minimum k for specimens of the same type from the same batch of concrete is used to present the range of the k value. The ratio for the cylinder specimens from batches B and D are higher than that for those cylinder specimens tested in the previous work [3]. The splitting tension cylinders tested in the previous work were all the regular cylinder specimens with no hole. Also, it can be seen that the hole drilled at the axis of the cylinder has increased the ratio for the splitting tension cylinders to be higher than the ratio for the beam specimens.

Conclusions

The peak-load method can be applied to the splitting tension cylinders to determine K_{Ic}^S and $CTOD_c$ of TPFM. The cylinder specimen with a hole drilled at its axis is considerably distinct from the cylinder specimen without a hole. Thus, testing of cylinders of both types from the same batch of concrete can raise the reliability of the results obtained by the peak-load method.

Experimental results indicate that the slope of the $CTOD_c - K_{Ic}^S$ curve of a specimen at the solution of K_{Ic}^S, designated as k, can be used to distinguish specimens in the sense of the peak-load method. With a large range of the k value, the curvature of the optimization function at the minimum of the function, designated as β, is large. A large β promises a reliable solution of K_{Ic}^S and $CTOD_c$. The k value is dependent on specimen geometry, specimen size, and length of initial notch. Specimens should be designed so as to have a large range of the k value in order to obtain a reliable solution.

Based on finite element analysis, LEFM formulas for K_I, $CMOD$, and COD profiles are obtained for the regular and holed splitting tension cylinders. Using these formulas, one can accurately determine K_{Ic}^S and $CTOD_c$ by using the peak-load method.

Appendix: Linear Elastic Fracture Mechanics Formulas for Three-point Bend Beam and Eccentric Compression Prism

(1) *Three-Point Bend Beam* ($l/d = 2.5$)

The stress intensity factor:

$$K_1 = \sigma_N \sqrt{\pi a} N(\alpha) \tag{A1}$$

$$\sigma_N = \frac{3Pl}{2bd^2} \tag{A2}$$

$$N(\alpha) = \frac{1}{\sqrt{\pi}} \frac{1.83 - 1.65\alpha + 4.76\alpha^2 - 5.3\alpha^3 + 2.51\alpha^4}{(1 + 2\alpha)(1 - \alpha)^{1.5}} \tag{A3}$$

where l is the span between the supports.

The crack mouth opening displacement ($CMOD$):

$$CMOD = \frac{4a\sigma_N}{E'} V(\alpha) \tag{A4}$$

$$V(\alpha) = 0.65 - 1.88\alpha + 3.02\alpha^2 - 2.69\alpha^3 + \frac{0.68}{(1 - \alpha)^2}. \tag{A5}$$

The crack opening displacement (COD):

$$\frac{COD(y)}{CMOD} = \sqrt{\left(1 - \frac{y}{a}\right)^2 + [1.081 - 1.149\alpha]\left[\frac{y}{a} - \left(\frac{y}{a}\right)^2\right]}. \tag{A6}$$

Equation A3 has been provided by Jenq and Shah [1] for the beam ($l/d = 4$). As the authors of this paper have checked, this equation is also valid for the beam ($l/d = 2.5$).

(2) *Eccentric Compression Prism*

The stress intensity factor:

$$K_I = \sigma_N \sqrt{\pi a} N_c(\alpha) \tag{A7}$$

where

$$\sigma_N = \frac{P}{bd} \tag{A8}$$

$$N_c(\alpha) = mN_1(\alpha) - N_2(\alpha) \tag{A9}$$

$$m = 3 + 6\frac{c}{d} \tag{A10}$$

$$N_1(\alpha) = 1.122 - 1.40\alpha + 7.33\alpha^2 - 13.08\alpha^3 + 14.0\alpha^4 \tag{A11}$$

$$N_2(\alpha) = 1.122 - 0.231\alpha + 10.55\alpha^2 - 21.71\alpha^3 + 30.382\alpha^4. \tag{A12}$$

The *CMOD:*

$$CMOD = \frac{4a\sigma_N}{E'}V_c(\alpha) \tag{A13}$$

where

$$V_c(\alpha) = [mV_1(\alpha) - V_2(\alpha)] \tag{A14}$$

$$V_1(\alpha) = 0.8 - 1.7\alpha + 2.4\alpha^2 + \frac{0.66}{(1-\alpha)^2} \tag{A15}$$

$$V_2(\alpha) = \frac{1.46 + 3.42(1 - cos\frac{\pi}{2}\alpha)}{\left(cos\frac{\pi}{2}\alpha\right)^2}. \tag{A16}$$

The *COD:*

$$\frac{COD(y)}{CMOD} = \sqrt{\left(1-\frac{y}{a}\right)^2 + \left[1.145 - 2.086\frac{a}{d} + 0.802\left(\frac{a}{d}\right)^2\right]\left[\frac{y}{a} - \left(\frac{y}{a}\right)^2\right]}. \tag{A17}$$

Equations A11 and A12 are provided by Tada et al. [7] and eq A13 results from the finite element computation by the authors of this paper.

References

1. Jenq, Y.S.; Shah, S.P. *J. Engin. Mech.* **1985,** *111,* 1227–1241.
2. RILEM Committee on Fracture Mechanics of Concrete—Test Method. *Mater. Struct.* **1990,** *23,* 457–460.
3. Tang, T.; Ouyang, C.; Shah, S.P. *ACI Mater. J.* **1996,** *93,* 147–157.
4. Tang, T.; Yang, S.; Ouyang, C.; Libardi, W.; Shah, S.P. *Fracture Mechanics of Concrete Structures,* Vol. 1; Wittmann, F.H. Ed.; AEDIFICATIO Publishers: Freiburg, Germany, **1995,** pp 135–144.
5. Karihaloo, B.L.; Nallathambi, P. *Mag. Concr. Res.* **1986,** *38,* 67–76.
6. Tang, T. *J. Testing Eval.* **1994,** *22,* 401–409.
7. Tada, H.; Paris, P.C.; Irwin, G.P. *The Stress Analysis of Cracks Handbook;* Paris Productions Inc.; St. Louis, MO, **1985;** pp 8–12.